Nuclear Inst. and Methods in Physics Research, A 957 (2020) 163401

Contents lists available at ScienceDirect

Nuclear Inst. and Methods in Physics Research, A

journal homepage: www.elsevier.com/locate/nima

Technical notes

PMT glass window sensitivity to gamma-rays: A digital signal processing approach

M. Ghahremani Gol [a,*], M. Khakzad [a], S. Jamili [a], N. Ghal-Eh [b,c]

[a] School of Particles and Accelerators, Institute for Research in Fundamental Sciences (IPM), P.O. Box 19395-5531, Tehran, Iran
[b] School of Physics, Damghan University, P.O. Box 36716-41167, Damghan, Iran
[c] Department of Physics, Faculty of Sciences, Ferdowsi University of Mashhad, P.O. Box 91775-1436, Mashhad, Iran

ARTICLE INFO

Keywords:
Photomultiplier tube (PMT)
Scintillation detector
Time response
Digital pulse processing

ABSTRACT

A digital data acquisition system together with MATLAB software for data analysis were utilised to measure the pulse specification of the scintillation detector assembly. Besides, the sensitivity of a photomultiplier tube (PMT) window to gamma-rays was studied to discriminate the signals produced as a result of gamma-ray interactions inside the glass window from those originating from the scintillator cell. The result showed that an algorithm based on the time features was capable to evaluate the contributions of these two different signals.

1. Introduction

The PMTs are the most appropriate tools for detecting visible, ultraviolet, and near-infrared radiations due to their high sensitivity, low-noise and fast response, which are widely used in different applications ranging from particle and nuclear physics to astronomy and space sciences [1]. In PMTs, the photons incident on the photocathode are converted to electrons which are further accelerated toward the first dynode before they are multiplied within the dynode chain whose potential differences are maintained by an appropriate voltage-dividing circuit [2].

Scintillation detectors are commonly used in various applications and radiation fields, from radioactivity measurements and imaging in industry and medicine to high-energy particle physics and astrophysics experiments [3–8]. When an ionising radiation passes through the scintillators, it interacts within the scintillator cell and produces secondary-charged particles (*e.g.*, electrons and protons as a result of gamma-rays and neutrons, respectively), whose partial deposition energies are further converted to a flash of visible or near-visible light. Since the scintillators are generally transparent to their own scintillation photons, these so-called optical photons easily reach to photosensitive region, the PMT, where they are converted to photoelectrons [1].

In a comprehensive work undertaken by Krall [9], it was observed that there were excess light generations for the detector exposed to low-energy gamma-rays and charged particles, for which the scintillation within the PMT glass window was believed to be the main reason. The scintillation in the PMT had been also confirmed by Anderson [10], where several PMT types where examined with proton beam irradiations. Moreover, the PMT glass window scintillation was studied by Bayat et al. [11] where they concluded that this effect was significant especially in low-efficiency scintillation detectors.

The glass window scintillation basically put a limit on the use of PMTs in some specific applications such as coincidence measurements, time-of-flight studies and intrinsic efficiency assessment [12]. Therefore, the discrimination of signals originating from the scintillator cell from those associated with the glass window is an essential task to undertake.

In general, the pulse-shape analysis of the PMT output signal provides unique information that can be used in energy sensitivity and fast time response measurements as well as particle type identification studies.

The time response of scintillators represent an exponential-decay form involving fast and slow components. A typical plastic scintillator time response is given in Eq. (1) [13], where $N(t)$ and τ are the number of optical photons generated at time t and decay time constant, respectively. $f(\sigma,t)$ represents a Gaussian with standard deviation σ.

$$N(t) = N_0 f(\sigma, t) exp(-t/\tau) \quad (1)$$

The rise time of a scintillator pulse is usually very short whilst the decay times may vary from one scintillator to another. The latter may be used in pulse-shape discrimination (PSD) by incorporating appropriate circuitry in case of organic compounds, although some research studies have identified the PSD properties of inorganics as well [14].

In the following section, the algorithm for the discrimination of the plastic scintillator response from that of PMT glass window by digital pulse-shape analysis is presented.

* Corresponding author.
E-mail address: m.ghahremani@ipm.ir (M. Ghahremani Gol).

https://doi.org/10.1016/j.nima.2020.163401
Received 8 October 2019; Received in revised form 30 December 2019; Accepted 5 January 2020
Available online 15 January 2020
0168-9002/

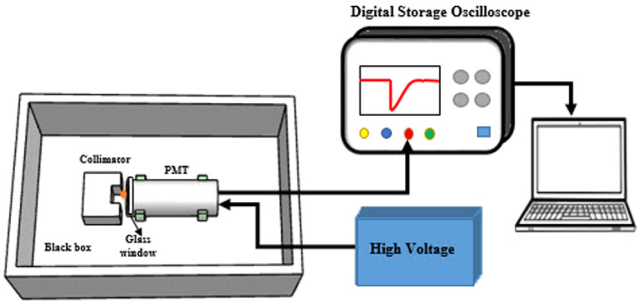

Fig. 1. The detection setup used for the glass window response measurement of the PMT with different glass materials.

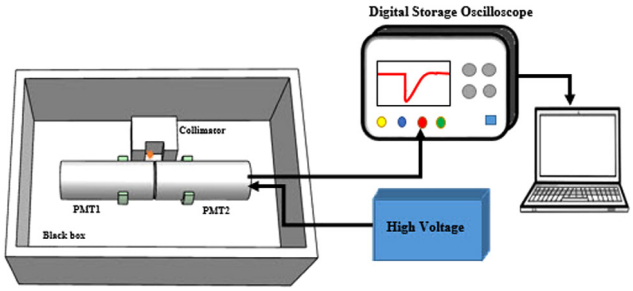

Fig. 2. The detection setup used for the glass window response measurement when a second PMT glass is optically coupled to the main one.

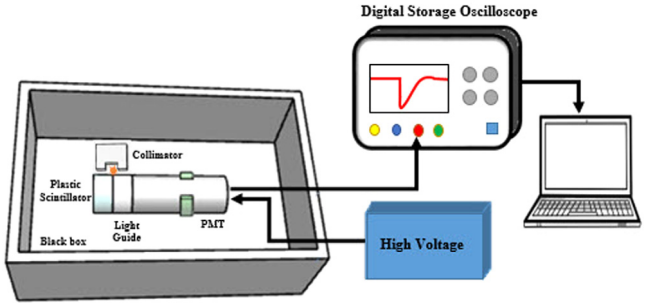

Fig. 3. The detection setup used for the measurement of a plastic scintillator signals.

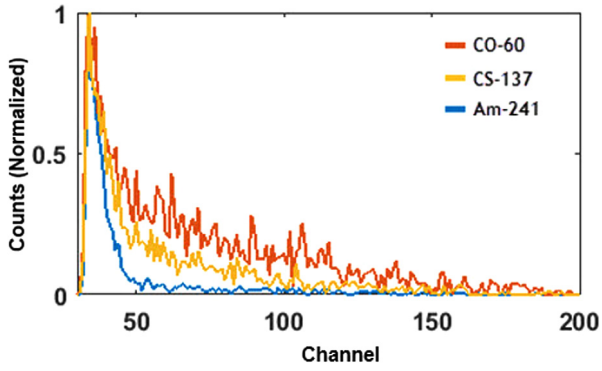

Fig. 4. The spectra measured with the PMT exposed to different radioactive sources.

2. Materials and methods

The block diagram of the proposed digital data-acquisition system used in three different setups are shown in Figs. 1–3. The measurement system consists of a 5.08 cm diameter by 5.08 cm long cylindrical NE102 plastic scintillator, two circular-face Photonis XP2020 PMTs [15] with 52-mm diameter borosilicate glass windows, N570 CAEN high-voltage power supply, an 8-bit GDS3504 GW Instek digital oscilloscope with 4 GS/s sampling rate and different radioactive gamma-ray sources (^{60}Co (1 μCi), ^{137}Cs (1 μCi), ^{241}Am (1 μCi)). The anode pulse of the PMT with an output impendence of 50 Ω is fed into the oscilloscope which operates as a digitiser throughout the measurements.

A data-logger software written in C# language has been responsible for the data acquisition from a GDS-3504 digital oscilloscope. Both the data acquisition rate and connection port have been preset. Then, the storage location of pulse data as well as the time intervals have been determined. At the output, every anode pulse has been stored in either .txt or .csv format in a two-column matrix. The data acquisition and analysis procedures were explained as following: (1) Mathematica [16] and MATLAB [17] softwares have been used for non-linear curve-fitting and plotting the PMT as well as the scintillator anode pulses, respectively. (2) Having investigated the amplitude, rise time, fall time and the FWHM of the anode pulses, it has been decided to choose the FWHM as the most appropriate factor to discriminate the PMT pulses from those originating from plastic scintillator. (3) MATLAB has been used to discriminate and plot both the PMT and plastic scintillator 3D data according to their different FWHM values. (4) Finally, the 2D spectra corresponding the PMT and plastic scintillator have been plotted separately by MATLAB.

Fig. 1 shows the measurement setup that might be used to study the scintillation and Cerenkov photons generated inside both the scintillator cell and the 3-mm thick glass doped with boron and iron in the form of well-known KB7 and Lime glasses, respectively. Note should be taken that the probability of scintillation light emission is considerably higher than Cerenkov in the gamma-ray energy range used in the present study [18]. Fig. 2 represents the setup in which an extra glass window with identical material composition has been added to the main one through an optical coupling in order to increase the scintillation light production probability within the PMT glass.

In order to discriminate the plastic scintillator pulse from the pulse originating from the PMT glass, two different data acquisition setups have been employed: (1) The measurement setup where the PMT without plastic scintillator is exposed to 1 μCi ^{137}Cs point source and (2) The measurement setup, as shown in Fig. 3, in which the detector assembly consisting the PMT and a plastic scintillator are attached through a 2-cm Plexiglass lightguide, both exposed to 1 μCi ^{137}Cs point source.

The detector output pulses have been acquired by a digital spectroscopy system before processing the data with MATLAB. Then, different pulse characteristics such as rise time, fall time and FWHM have been extracted and processed. Finally, the output pulses originating from both the plastic scintillator and the PMT glass have been identified and discriminated.

3. Results and discussion

The spectra obtained from the detector with a bare PMT (*i.e.*, without scintillator cell) when exposed to different point sources confirm the PMT sensitivity to both gamma-rays and the source type (See Fig. 4).

The count rates of the PMT output pulses measured with a bare PMT, with and without extra glasses, when exposed to ^{60}Co point source are listed in Table 1. The voltage threshold for the counts measurements has been set as 20 mV.

As it can be seen in Table 1, the count rate increases considerably with the addition of an extra glass to the PMT window and also it varies with the type of PMT glass.

In order to select the output pulses due to the PMT glass scintillations and those from a PMT with the plastic scintillator, the data acquisitions have been made for 12 h based on the measurement setups

Table 1
The output signal count rates measured with the PMT of different glass window conditions.

PMT glass window condition	Source	Count rates
PMT without extra glass	BG[a]	30
	^{60}Co	200
PMT with extra glass (*i.e.*, two coupled PMTs)	BG	120
	^{60}Co	800
PMT with BK7 glass	BG	70
	^{60}Co	330
PMT with Lime glass	BG	55
	^{60}Co	225

[a]BG stands for background count rates.

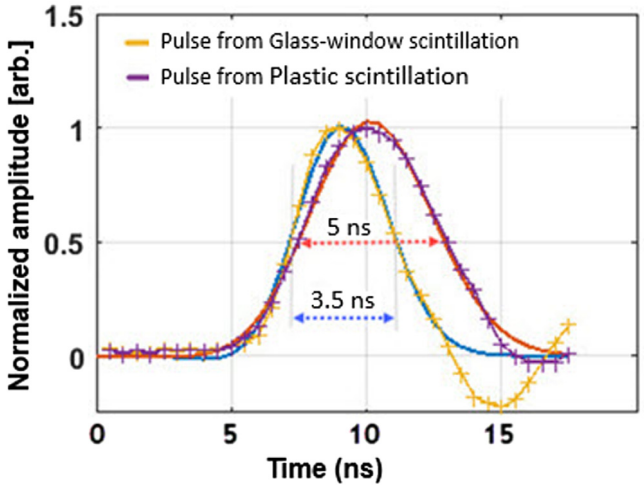

Fig. 5. The normalised PMT signals corresponding to the PMT glass window and the plastic scintillator.

shown in Figs. 1 and 3. The statistical analyses undertaken on the output pulse characteristics (*i.e.*, rise time, fall time and FWHM) showed that the majority of output pulses obtained from the measurement setup of Fig. 1, which represent the bare PMT output pulses, have the FWHM of less than 4 ns.

However, the pulses obtained from setup 2, which represent the PMT output pulses of the detector with the plastic scintillator, include the pulses with the FWHMs both less than and greater than 4 ns.

Fig. 5 illustrates sample output pulses generated from the PMT glass window scintillation along with those from plastic scintillator.

The detector output pulses when the PMT is with or without the plastic scintillator, as shown in Fig. 5, may be modelled through a Levenberg–Marquardt non-linear curve fitting of the following function (see Table 2):

$$F(x) = P_1 e^{-\frac{(-P_2+x)^2}{P_3^2}} (e^{P_4 x} + P_6 e^{P_5 x}). \quad (2)$$

As one may expect, the identification and discrimination of the detector pulses produced in the assembly, with and without plastic scintillator, can be easily undertaken in terms of the FWHM values as shown in Fig. 5.

The pulses originating from the PMT represents low amplitudes due to the low scintillation efficiency of the glass window, except those corresponding to high-energy cosmic rays, however, the plastic scintillator pulse-heights are relatively large.

Fig. 6 shows a three-dimensional discrimination plot of the plastic-scintillator-induced pulses versus those from PMT glass, using response function difference method. Whilst, the same discrimination plot for the assembly without plastic scintillator is shown in Fig. 7.

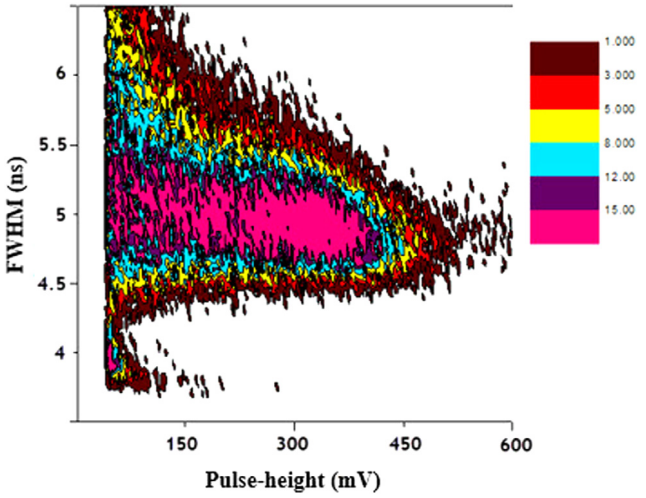

Fig. 6. A 3D illustration of the scintillation detector pulses, where the discrimination was made in terms of different pulse FWHMs.

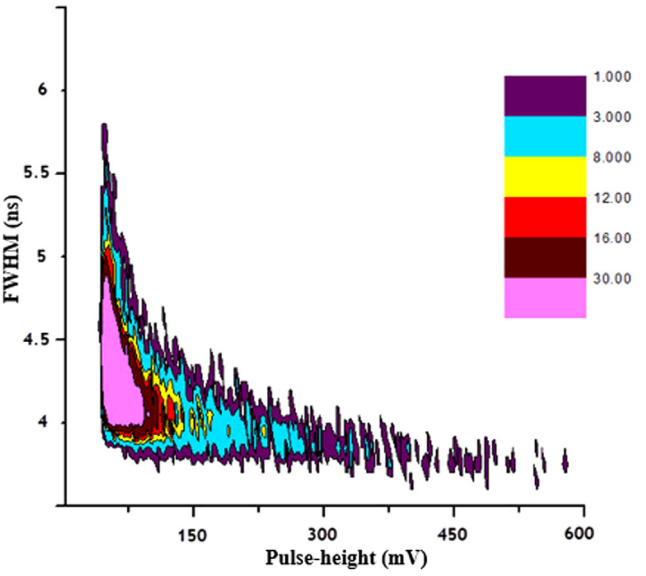

Fig. 7. A 3D illustration of the glass window scintillation pulses for a detector without plastic scintillator using the proposed algorithm.

The measured spectra shown in Fig. 8 correspond to the detector exposed to ^{137}Cs when both the PMT glass and scintillator cell contributions to the detector signal are taken into account as well as the discriminated spectra, where the two components are illustrated separately. As it can be seen, the discriminated spectrum is in agreement with the spectrum measured in bare PMT case.

4. Conclusions

According to measurement data listed in Table 1, the major factor in PMT sensitivity is the glass window scintillation. As it can be seen, by adding a 3-mm thick extra glass to the PMT window, the count rate has increased from about 15 to 60 percent depending on the type and thickness of the glass. If the extra glass coupled to the PMT window is made of the same material as the glass window, the count rate exhibits a four-times increase.

Moreover, the time response of the PMT glass is considerably different from that of the plastic scintillator, where the discrimination can be simply made using the time features (e.g., FWHM). The FWHMs of the

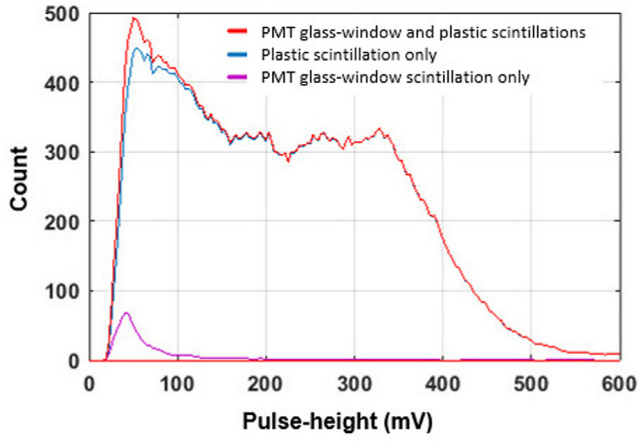

Fig. 8. The measured spectra for the detectors with and without plastic scintillator when exposed to ^{137}Cs source along with the discriminated spectra.

Table 2
Fitting parameters calculated for the PMT output signals when the detector is with and without plastic scintillator.

Fitting parameters	PMT with plastic scintillator	PMT glass window
P1	1.582	1.561
P2	18.573	16.854
P3	4.477	5.165
P4	−0.047	0.017
P5	0.031	−0.066
P6	−0.576	−2.251

output pulses from the detector, may be categorised into below and above 4 ns. The pulses originating from the glass window scintillation, for example, are corresponding to those with FWHMs lass than 4-ns. This discrimination capability is important in different applications such as time-of-flight and response function measurements when both scintillation and Cerenkov light may be present. The results confirm that the PMT coupled to a plastic scintillator may be regarded as a phoswich detector for an α-γ source (e.g., ^{241}Am), where a very thin plastic scintillator and the PMT glass window operate as alpha and gamma-ray spectrometers, respectively.

Acknowledgements

We would like to thank Professor Mojtaba Mohammadi Najafabadi and Dr. Behzad Boghrati from IPM, Iran, for their cooperation and the provision of the measurement equipments. We are also grateful to Dr. Aldo Penzo from CERN, Switzerland, for giving us some instruments and to Dr. Ewart Blackmore from TRIUMF, Canada, for his fruitful discussion and help.

References

[1] G.F. Knoll, Radiation Detection and Measurement, John Wiley & Sons, 2010.
[2] www.hamamatsu.com.
[3] C.W. van Eijk, Inorganic scintillators in medical imaging, Phys. Med. Biol. 47 (8) (2002) R85.
[4] D.V. Jordan, P.L. Reeder, L.C. Todd, G.A. Warren, K.R. McCormick, D.L. Stephens, B.D. Geelhood, J.M. Alzheimer, S.L. Crowell, W.A. Sliger, Advanced Large Area Plastic Scintillator Project (ALPS) (No. PNNL-17305), Pacific Northwest National Lab. (PNNL), Richland, WA (United States), 2008.
[5] N. D'Ascenzo, V. Saveliev, The new photo-detectors for high energy physics and nuclear medicine, in: Photodiodes-Communications, Bio-Sensings, Measurements and High-Energy Physics, IntechOpen, 2011.
[6] S. Stefanowicz, H. Latzel, L.R. Lindvold, C.E. Andersen, O. Jäkel, S. Greilich, Dosimetry in clinical static magnetic fields using plastic scintillation detectors, Radiat. Meas. 56 (2013) 357–360.
[7] R.S. Perea, A.M. Parsons, M. Groza, D. Caudel, S.F. Nowicki, A. Burger, K.G. Stassun, T.E. Peterson, Scintillation properties of strontium iodide doped with europium for high-energy astrophysical detectors: nonproportionality as a function of temperature and at high gamma-ray energies, J. Astron. Telesc. Instrum. Syst. 1 (1) (2014) 016002.
[8] P. Maoddi, Microfluidic Scintillation Detectors for High Energy Physics (No. THESIS), EPFL, 2015.
[9] H.R. Krall, Extraneous light emission from photomultipliers, IEEE Trans. Nucl. Sci. 14 (1) (1967) 455–459.
[10] K.A. Anderson, Luminescent effects in photomultiplier tube faces and Plexiglas Cerenkov detectors, Rev. Sci. Instrum. 30 (10) (1959) 869–873.
[11] E. Bayat, V. Doust-Mohammadi, P. Ghorbani, N. Ghal-Eh, R. Mohammadi, Scintillation of XP2020 PMT glass window, Radiat. Phys. Chem. 102 (2014) 1–4.
[12] F.A. Johnson, Investigation of source-dependent contributions to photomultiplier noise, Nucl. Instrum. Methods 87 (2) (1970) 215–220.
[13] W.R. Leo, Techniques for Nuclear and Particle Physics Experiments: A How-to Approach, Springer Science and Business Media, 2012.
[14] Y. Ashida, H. Nagata, Y. Koshio, T. Nakaya, R. Wendell, Separation of gamma-ray and neutron events with CsI (Tl) pulse shape analysis, Prog. Theor. Exp. Phys. 2018 (4) (2018) 043H01.
[15] www.photonis.com.
[16] www.wolfram.com/mathematica.
[17] www.mathworks.com/products/matlab.html.
[18] E. Roncali, S.I. Kwon, S. Jan, E. Berg, S.R. Cherry, Cerenkov light transport in scintillation crystals explained: realistic simulation with GATE, Biomed. Phys. Eng. Express 5 (3) (2019) 035033.